

The Vaporization-Controlled Inertial Regime in Nonpremixed Counterflow Spray Combustion

Jaime Carpio, Amable Liñán
Universidad Politécnica de Madrid
Madrid, Spain

Daniel Martínez-Ruiz
Universidad Carlos III de Madrid
Leganés, Spain

Antonio L. Sánchez, Forman A. Williams
University of California, San Diego
La Jolla, CA, USA

1 Introduction

Improvements in understanding of combustion processes for fuel sprays in nonuniform flows are needed for advancing engine technologies that employ liquid fuels. Comprehension can be enhanced by identifying different combustion regimes on the basis of appropriate nondimensional parameters and studying how the combustion occurs in each regime. The Stokes number of the droplets in the spray is a key parameter affecting the combustion process. By focusing on nonpremixed counterflow configurations as representative of sprays for many applications, it has recently been shown that, in addition to the known regime at small Stokes numbers, in which nonpremixed spray combustion occurs in the mixing layer between an oxidizer gas stream and a stream of inert gas carrying the fuel droplets, there is a vaporization-controlled inertial regime at Stokes numbers of order unity and larger, in which the droplets penetrate into the oxidizer stream because of their higher inertia and vaporize there, leading to the combustion occurring well into the oxidizer stream [1]. Since the combustion characteristics are poorly understood for that regime, the present work employs numerical methods to help to clarify flame structures that may arise there. It will be shown that, perhaps unexpectedly, when the Stokes numbers reach values on the order of $St \simeq 3$ or greater, a cold fuel stream impinging on a hotter air stream may exhibit two very different types of steady-state combustion behavior, depending on how the interaction process is initiated. The characteristics of each of these will be shown, as well as the characteristics of combustion in the vaporization-controlled inertial regime at Stokes numbers below those at which the dual solutions are obtainable.

It is widely accepted that canonical problems are useful in understanding the interplay of the physicochemical processes that arise in spray–combustion applications [2, 3]. The counterflow configuration investigated here, which serves as a local model for investigating strained diffusion flames in turbulent environments [4], has been widely used by the combustion community, in both experiments [5, 6] and numerical investigations [7–13]. The present numerical study then will focus on analysis of influences of droplet inertia on the resulting spray flames, with particular attention given to the recently discovered vaporization-controlled inertial regime [1], which currently is the least understood regime.

2 The model problem

The specific problem addressed concerns the axisymmetric flow arising from the collision of two large-Reynolds-number gaseous jets, one of hot air and the other of an inert gas (e.g. nitrogen) carrying a monodisperse spray of fuel droplets, as may model processes that occur in liquid-fueled gas-turbine or internal-combustion engines, for example. Attention is focused on the region near the stagnation point of two opposed potential-flow streams, where the gas velocity is determined by the uniform strain rate found on each side of the stagnation plane. On the spray side the velocity field $\mathbf{v} = (u, v)$ is given by

$$u = -A_s z \quad \text{and} \quad v = A_s r/2,$$

where u and v are the axial and radial velocity components, and A_s is the spray-side strain rate. The corresponding strain rate on the air side is, in general, different, with a value $A_A = A_s(\rho_s/\rho_A)^{1/2}$ dictated in terms of the spray-to-air density ratio ρ_s/ρ_A by the condition of a negligible axial pressure jump.

The formulation used in the numerical integrations, omitted here because of space limitations, parallels those given earlier [1, 3]. Besides addressing the limit of infinitely fast chemistry, with use made of chemistry-free coupling functions that allow for a general nonunity Lewis number L_F of the fuel vapor [1, 3], a one-step irreversible Arrhenius reaction between the oxygen in the air and the fuel vapor is considered, with an activation temperature T_a and a characteristic inverse chemical time B , this rate being proportional to the product of the gas-phase fuel mass fraction Y_F and the oxygen concentration Y_{O_2} , the value of which in the air stream is $Y_{O_2,A} = 0.232$. Important quantities for the analysis are the mass of air needed to burn the unit mass of fuel S typically lying between five and twenty, and the amount of heat released per unit mass of fuel consumed Q , which can be normalized by the product of the specific heat at constant pressure for the gas, c_p with the boiling temperature T_B of the liquid fuel. Droplet vaporization rates are related to Y_F and the droplet radius a by the classical formula, with the fuel-vapor mass fraction at the droplet surface related to the droplet temperature T_d by the Clausius-Clapeyron relation involving the heat of vaporization per unit mass L_v and the fuel gas constant per unit mass, R_F . In the computations, the initial droplet temperature is set equal to that of the carrier gas, $T_s = 300$ K, which is also used to scale the boiling temperature. Calculations were performed for both methanol and dodecane, with properties given in Table 1.

Table 1: Main dimensionless properties of methanol and dodecane fuels

	S	L_F	c_p/R_F	T_B/T_s	$L_v/(R_F T_B)$	$Q/(c_p T_B)$
Methanol	6.5	1.2	3.85	1.123	12.58	59.15
Dodecane	15	3.6	24.54	1.630	15.21	75.83

3 Controlling parameters in counterflow spray diffusion flames

The droplets are assumed to be injected with a temperature $T_d = T_s < T_B$ at distances from the stagnation plane z_I much larger than the mixing-layer thickness $\delta_m = (D_{T_s}/A_s)^{1/2}$ (based on the thermal diffusivity of the unperturbed carrier gas D_{T_s}), with the square of their ratio

$$Pe = \left(\frac{z_I}{\delta_m} \right)^2 = \frac{z_I^2 A_s}{D_{T_s}} \quad (1)$$

defining the relevant Peclet number, a moderately large parameter in the description.

Attention is focused on dilute sprays, typically found in the main vaporization and combustion region of practical liquid-fueled combustion devices [2, 3], where the interdroplet distances are significantly larger than the droplet diameter and, for the counterflow configuration, smaller than the mixing-layer thickness δ_m . The two main parameters describing the interphase coupling in counterflow sprays are the Stokes number

$$St = \frac{2 a_I^2 \rho_l}{9 \mu_s} A_s \quad (2)$$

defined as the ratio of the droplet acceleration time $\frac{2}{9} a_I^2 \rho_l / \mu_s$ to the mixing-layer strain time A_s^{-1} , and the spray liquid mass-loading ratio at the injection plane

$$\alpha = \frac{(4\pi/3) a_I^3 n_I \rho_l}{\rho_s} \quad (3)$$

Here ρ_s and μ_s are the density and viscosity of the carrier gas, ρ_l is the density of the liquid fuel, and a_I and n_I are the droplet radius and number of droplet number density at the injection plane. As discussed in [1], in nonreacting spray flows the Stokes number measures the coupling of the droplets with the gas flow, while the ratio α/St measures the coupling of the gas phase with the droplets, so that effective two-way coupling occurs in the double distinguished limit $St \sim 1$ and $\alpha \sim 1$. The coupling is more pronounced in the presence of combustion, because the heat released by oxidation of the fuel vapor is enough to lead to flame temperatures several times larger than the spray feed temperatures. Since S is approximately $S = 15 \gg 1$ for typical hydrocarbon fuels, very dilute sprays with relatively small values of $\alpha \sim S^{-1} \ll 1$ may generate diffusion-flame temperatures of the order of the stoichiometric adiabatic flame temperature, thereby producing a strong effect on the gas flow through the associated gas expansion.

4 Results and Discussion

For values of St below a critical value St_c , which is seen to be $St_c = 1/4$ for dilute sprays with small values of the spray liquid mass-loading ratio $\alpha \sim S^{-1} \ll 1$, the droplets decelerate to approach the gas stagnation plane with a vanishing axial velocity [1]. In this case, the droplets located initially near the axis reach the mixing layer, where they can vaporize due to the heat received from the hot air, producing fuel vapor that can burn with the oxygen in a diffusion flame embedded in the mixing layer. The behavior at higher Stokes numbers is quite different from that, as shown in Figs. 1 and 2, which represent results of computations performed for $\alpha = 0.05$ and $Pe = 100$, obtained as the steady solutions reached in transient computations after a sufficiently long integration time. The droplets now cross the stagnation plane and move into the opposing air stream, reaching distances of order $z_I \gg \delta_m$ before they turn around. The vaporization of

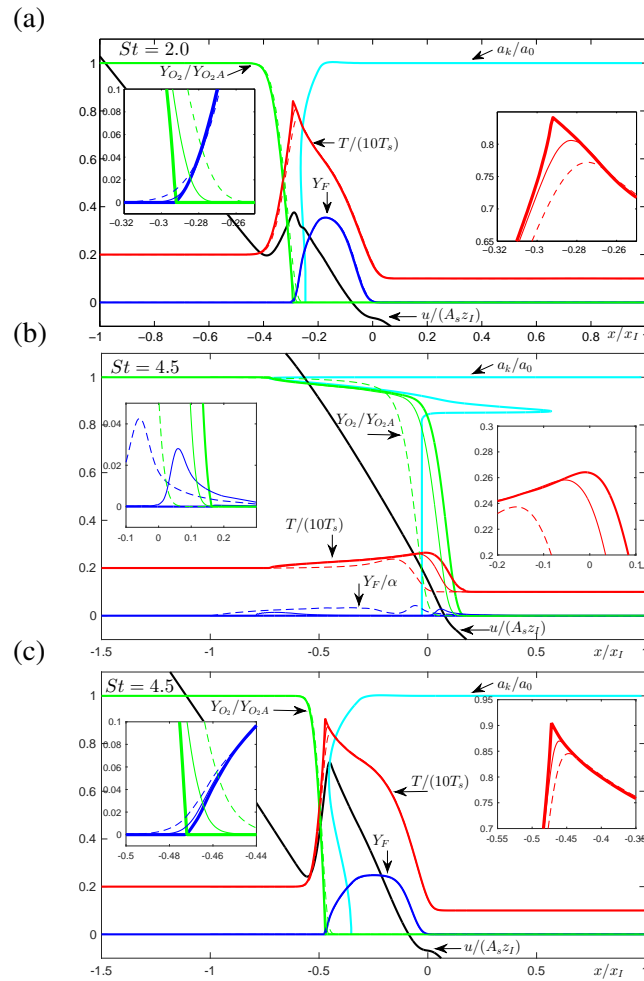


Figure 1: Profiles of reactant mass fractions, temperature, transverse velocity, and droplet radius obtained for dodecane by numerical integration with infinitely fast reaction (thick solid curves) and with an Arrhenius rate for $T_a/T_s = 30$ and $B/A_s = 10^5$ (thin dashed curves) and $B/A_s = 10^6$ (thin solid curves).

these crossing droplets, and also the combustion of the fuel vapor generated by them, occur in the hot air stream, without significant effects of molecular diffusion, generating a vaporization-assisted nonpremixed flame that stands on the air side outside the mixing layer [1].

The first figure has three parts, the first for a Stokes number at which only one solution exists, and the second and third for a value at which two solutions exist, showing each of these solutions. Fig. 1a corresponds to a dodecane flame for $St = 2$. As can be seen in the profile of droplet radius, vaporization occurs primarily near the flame, with the droplets disappearing abruptly soon after turning around. The solutions shown here for different values of the reaction rate indicate that, as expected, the results with finite-rate chemistry approach for increasing Damköhler numbers B/A_s those obtained with infinitely fast chemistry.

The two solutions shown for the higher value of the Stokes number are quite different. Instead of a robust flame with a pronounced temperature peak, combustion occurs in a flameless mode, with the fuel vapor generated from the vaporizing droplets burning in a distributed manner with the surrounding oxygen. The

structure of this solution is illustrated in Fig. 1b. Because of the relatively low temperature, the droplets cross the stagnation plane a number of times before vaporizing completely. The comparison of the different curves in Fig. 1b reveals that the fuel vapor appears in decreasing amounts for increasing values of the Damköhler number B/A_s , and it disappears altogether in the limit of infinitely fast chemistry.

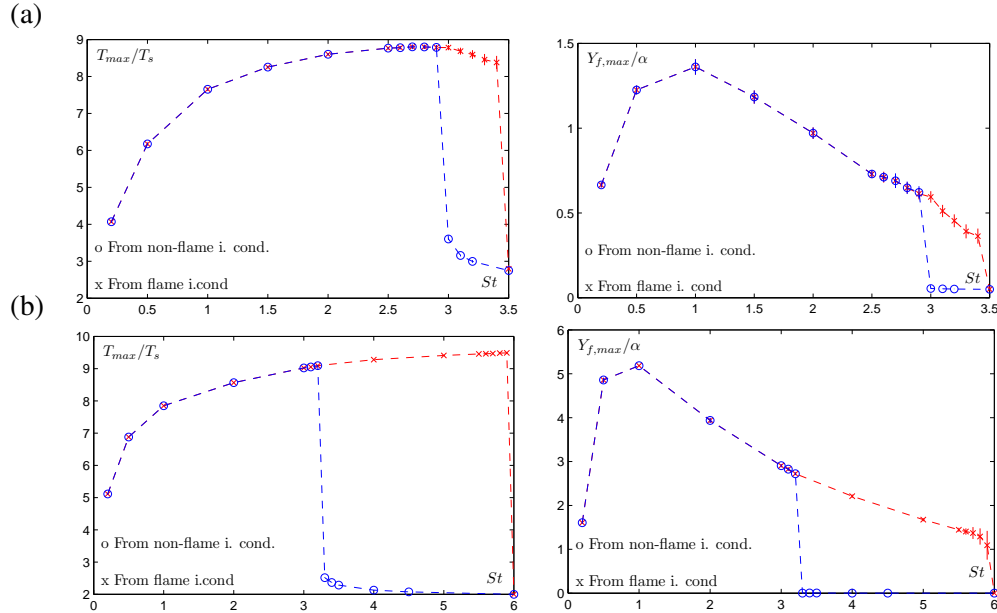


Figure 2: The variation with the Stokes number of the peak temperature and peak fuel mass fraction of the steady solution for methanol (a) and dodecane (b) obtained by initiating the integration from a chemically frozen state (circles) and from a flame (crosses).

While thin flames are the only combustion solution found for St below a limiting value (e.g. $St < 3.2$ for dodecane) and flameless combustion is the only solution found for St sufficiently large (e.g. $St > 6.0$ for dodecane), there exists an intermediate range of Stokes numbers in which the spray-flame problem admits both types of solutions, which can be described in the transient numerical integrations by appropriately selecting as initial condition either a Burke-Schumann flame or a chemically frozen vaporizing spray. For instance, for $St = 4.5$, in addition to the flameless solution of Fig. 1b, there exists a thin-flame solution, shown in Fig. 1c.

Figure 2 summarizes results for both fuels, showing the ranges of multiplicity as functions of the Stokes number, obtained with the formulation for infinite reaction rates. Since the multiplicity appears even for infinitely fast chemistry, its existence can be attributed to the pronounced nonlinear effect associated with the strong temperature sensitivity of the vaporization rate through the large value of the dimensionless latent heat of vaporization $L_v/(R_F T_B)$. Since the initial droplet temperature is assumed in the computations to be $T_d = T_s$, the effect can be expected to be more pronounced for large values of T_B/T_s , for which the droplet vaporization rate in the carrier stream is found to be exponentially small. This claim seems to be supported by the numerical integrations, which reveal that the range of St for coexistence of the two solutions is larger for dodecane $T_B/T_s = 1.63$ than it is for methanol $T_B/T_s = 1.123$.

5 Conclusions

These results reveal that a surprising variety of different kinds of combustion behavior can exist in the vaporization-controlled inertial regime. Future work may better categorize the ranges of parameters over which these various types of combustion behavior may be encountered and the experimental conditions needed to produce them.

References

- [1] Liñán A, Martínez-Ruiz D, Sánchez AL, Urzay J. (2015). Regimes of spray vaporization and combustion in counterflow configurations. *Combust. Sci. Tech.* 187: 103.
- [2] Sirignano WA. (2010). *Fluid dynamics and transport of droplets and sprays*. Cambridge University Press.
- [3] Sánchez AL, Urzay J, Liñán A. (2015). The role of separation of scales in the description of spray combustion. *Proc. Combust. Inst.* 35: 1549.
- [4] Peters N. (2000). *Turbulent combustion*. Cambridge University Press (ISBN 0521660823)
- [5] Li SC. (1997). Spray stagnation flames. *Prog. Ener. Combust. Sci.* 23: 303.
- [6] Li SC, Williams FA. (2000). Counterflow heptane flame structure. *Proc. Combust. Inst.* 28: 1031.
- [7] Continillo G, Sirignano WA. (1990). Counterflow spray combustion modeling. *Combust. Flame* 81: 325.
- [8] Gao LP, D'Ángelo Y, Silverman I, Gomez A, Smooke MD. (1996). Quantitative comparison of detailed numerical computations and experiments in counterflow spray diffusion flames. *Proc. Combust. Inst.* 26: 1739.
- [9] Massot M, Kumar M, Smooke MD, Gomez A. (1998). Spray counterflow diffusion flames of heptane: experiments and computations with detailed kinetics and transport. *Proc. Combust. Inst.* 27: 1975.
- [10] Schlotz D, Gutheil E. (2000). Modeling of laminar mono- and bidisperse liquid oxygen/hydrogen spray flames in the counterflow configuration. *Combust. Sci. Tech.* 158: 195.
- [11] Kee RJ, Yamashita K, Zhu H, Dean AM. (2011). The effects of liquid-fuel thermophysical properties, carrier-gas composition, and pressure, on strained opposed-flow non-premixed flames. *Combust. Flame* 158: 1129.
- [12] Zhu H, Kee RJ, Chen L, Cao J, Xu M, Zhang Y. (2012). Vaporization characteristics of methanol, ethanol and heptane droplets in opposed stagnation flow at low temperature and pressure. *Combust. Th. Modelling* 16: 715.
- [13] Wang C, Dean AM, Zhu H, Kee RJ. (2013). The effects of multicomponent fuel droplet evaporation on the kinetics of strained opposed-flow diffusion flames. *Combust. Flame* 160: 265.